Induction Heating of Semisolid Billet and Control of Globular Microstructure to Prevent Coarsening Phenomena

H.K. Jung, C.G. Kang, and Y.H. Moon

(Submitted 20 August 1999; in revised form 18 October 1999)

An important step in the thixoforming process is the induction heating of the raw materials to the semisolid state. Using this technology, the process behavior is satisfactory from the point of view of reproducibility and temperature control. Therefore, the objectives of this study are to define the correct relationship between coil length and billet length for uniform induction heating and to present the optimal reheating conditions suitable for the thixoforming process (or to secure a fine globular microstructure without liquid segregation).

The optimal inductive coil on the induction heating process of semisolid billet machined to 76 mm diameter and 90 mm length to reduce the temperature gradient of the billet and to obtain the globular microstructure was theoretically designed and the suitability of the designed coil dimensions verified by reheating experiments.

The globular microstructures of semisolid billet in heating and holding processes were controlled to prevent the coarsening phenomena of Al-7%Si-0.3%Mg alloy and to apply to the thixoforming process. In addition, the effects of the history of processing and induction heating parameters such as reheating time, holding time, holding temperatures, capacity of the induction heating system, and adiabatic material size on the globularization were investigated.

It was concluded that in the case of a three-step reheating process, the final holding time is the most important factor and 2 min is suitable to maintain a globular microstructure.

Keywords coarsening phenomena, control of globular microstructure, final holding time, induction heating, optimal inductive coil, thixoforming

1. Introduction

The process of forming a partially melted nondendritic alloy billet within metal dies has been termed thixocasting, thixoforging, or, more generally, thixoforming. Thixoforming is a new method for forming billets in the semisolid state into net-shaped products. This method relies on the microstructural control of semisolid billets in which the solid phase exists in the form of spheroidal particles, and it has many advantages compared to die casting, squeeze casting, and conventional forging.[1–5]

From this point of view, the reheating conditions used to obtain a fine globular microstructure without liquid segregation are very important.[2–5] Moreover, the reheating of the billet in the semisolid state as quickly and homogeneously as possible is one of the most important parts of the process. To obtain the globular microstructure in a cross section of the billet, an optimal inductive coil design is necessary.[2–5]

In a study on the reheating process of semisolid material (SSMs), Young and Fitze[6] performed multistep reheating experiments by using induction systems with the capacity of 1 kW per unit time and unit kilogram; induction systems were attached to the circular conveyers. Kapranos *et al.*[7] compared the numerical results with the temperature of the five points in experiments with heating, soaking, and power-off stages. Kahrmann *et al.*[8] carried out the reheating experiments to heat for 300 to 350 from room temperature to 570 °C, ±5 °C. The billet size was 75 mm in diameter and 180 mm long. However, the accuracy of globularization was not investigated. Kang *et al.*[9] proposed the optimal reheating conditions to apply to the thixoforming process by using SSM billets with $d \times l = 39 \times 85$ mm and $d \times l = 76 \times 60$ mm. Jung and co-workers[2–5] proposed solutions for avoiding the coarsening phenomena of the Al-6%Si-3%Cu-0.3%Mg (ALTHIX 86S) alloy during induction heating and performed the numerical simulation of the induction heating process with an optimal coil design.

For the thixoforming process, the feeding and handling of the reheated billets are important in preventing temperature drop and maintaining the shape of the billet. Clauser *et al.*[10] have been studying the repeatability of the reheating process and the prevention of the attachment of the billet surface to the grip, which they have been performing using a robot with 7 degrees of freedom before and after the reheating process. EFU GmbH (Lammersdorf, Germany) constructed facilities to produce 25 aluminum billets per hour for billets of 100 mm diameter and 250 mm length by using four induction coils, and the billets are fed using an automatic feeding device.[11]

The influence of induction heating parameters such as reheating time, billet size, and holding temperature on the globular microstructure and coarsening phenomena has not been studied. In the present study, to determine the effects of the reheating conditions for the thixoforming process on the globularization of the

H.K. Jung, C.G. Kang, and **Y.H. Moon,** School of Mechanical Engineering, Engineering Research Center for Net Shape and Die Manufacturing, Pusan National University, Pusan 609-735, Korea.

microstructure, the reheating time (t_a), holding temperature (T_h), holding time (t_h), adiabatic material size, and capacity of the induction heating system (Q) were considered as parameters of the globularization of the microstructure. The present article concentrates on the optimal coil design needed to reduce the temperature gradient of the billet and to obtain a fine globular microstructure and the design's verification by reheating experiments.

2. The Characteristic Features of Inductive Heating

Induction heating has advantages over conventional electric furnace heating in that the former reduces the amount of scaling and scrap because it requires less billet heating time. The induction heating method can reduce scaling from 3 to 4% in a conventional furnace to 0.5%. In induction heating, the relationship between time and temperature must be controlled exactly to obtain a uniform temperature distribution over entire cross-sectional area.[2–5,12,13] Because the initial eutectic temperature (*i.e.*, initial solid fraction) is the key parameter in the thixoforming process, an accurately controllable induction heating method must be selected as the reheating process.

3. The Goals of Inductive Coil Design

For the thixoforming process, the reheating of the billet in the semisolid state as quickly and homogeneously as possible is one of the most important parts of the process. From this point of view, the design of the induction coil is very important. For a real system consisting of coil and billet, the induced heat over the length of the billet is normally not equally distributed, and consequently, there is a nonuniform temperature distribution. So an important point for optimization of coil design is to verify the correct relationship between coil length and billet length.[2–5,13] So, in this study, the optimal induction coil of the commercial induction heating system (for semisolid forming, 60 Hz) to obtain the globular microstructure for variations of the SSM and specimen size (diameter and length) was designed.

4. Theoretical Coil Design for Uniform Heating

For uniform reheating in this study, the optimal coil length H and coil inner diameter D_i of the induction heating system were designed, as shown in Fig. 2.

To consider the main surface power loss in induction heating, the idealized power density (P_s) must be represented as the actual power density (P_a), which is modified to allow for the ratio ($d/2\delta_F$) of a finite current depth of penetration (δ_F) of material and billet diameter (d).

$$\delta_F = \sqrt{\frac{2\rho_a}{\mu\omega}} \quad \text{(Eq 1)}$$

$$P_a = \frac{P_s(\theta_s - \theta_c)\ idealized}{\theta_s - \theta_c} = \frac{6.46\kappa(\theta_s - \theta_c)}{d} \quad \text{(Eq 2)}$$

In Eq 2, $\frac{(\theta_s - \theta_c)}{(\theta_s - \theta_c)_{idealized}} = k$ can be obtained from the variation curves of temperature in a cylinder with finite current depth of penetration[14] where ρ_a, μ, ω, κ, and $\theta_s - \theta_c$ are the resistivity of A356, the magnetic constant, the angular frequency, the thermal conductivity, and the maximum surface-center temperature difference, respectively.

If the production rate is assumed to be 90 mm height-10 billets heating per unit hour, the temperature rises to 584 °C, because, by Stansel's[15] data (in the case of a temperature rise to 510 °C, the thermal capacity of q = 145 kW h/t, and the production rate of P_r =0.01 t/h) and linear interpolation, the thermal capacity q and the production rate P_r are calculated, and the minimum heated surface area A_s and the minimum heated length l_w can be determined as follows:

$$A_s = \frac{P_t}{P_a} = \frac{P \times q}{P_a} \quad \text{(Eq 3)}$$

$$l_\omega = \frac{A_s}{\pi d} \quad \text{(Eq 4)}$$

To determine the coil inner diameter D_i and optimal coil length H, recommended air gaps [1/2 ($D_i - d$)] for through-heating coils and property values to calculate the optimal coil length are shown in Tables 1 and 2, respectively.

Table 1 Recommended air gaps [1/2 ($D_i - d$)] for through-heating coils[14]

		Billet diameter (d, mm)		
Frequency	**Billet temperature (°C)**	**0–60**	**60–125**	**125–250**
50/60 Hz	550	12	12	12
	850	12	20	40.4

Table 2 Property values to calculate the optimal coil length (f = 60 Hz, dc = 10.7 mm,[16] l = 90 mm, and k = 0.62)

Parameter	Symbol	Unit	Value	Reference
Maximum surface-center temperature difference	$\theta_s - \theta_c$	K	5	...
Thermal conductivity	κ	W/m K	159	17
Idealized power density	P_s	kW/m⁴	41.85	...
Resistivity of A356	ρ^a	$\mu\ \Omega$m	0.0421	17
Magnetic constant	μ	H/m	$4\pi \times 10^{-3}$	14
Angular frequency	ω	rad/s	120π	...
Finite current depth of penetration	δ_F	m	1.3×10^{-4}	...
Actual power density	P_a	kW/m⁴	67.5	...
Thermal power	P_t	kW	1.5	...
Production rate	P_r	Dimensionless	0.01 t/h	15
Thermal capacity minimum heated surface	q	kW	150 h/t	...
Area	A_s	m⁴	22.2×10^{-3}	...
Billet diameter	d	mm	76	...
Minimum heated length	l_w	mm	93	...

By using linear interpolation with Table 1, the coil inner diameter D_i is calculated, and from the result of Eq 4, the optimal coil length H can be calculated by Eq 5.

$$H = l_{\omega} + (25 \text{ to } 75) \quad \text{(Eq 5)}$$

Therefore, from the above considerations, the coil dimensions for the SSM with $d \times l = 76 \times 90$ mm can be proposed as in Table 3, and the experiments of induction heating are carried out by using those dimensions. The suitability of an optimal coil design was verified through the numerical simulation of the induction heating process by using a general purpose finite element code, ANSYS.[4,13] From the results of CAE, a coil length of 120 mm was most suitable from the point of view of minimizing the electromagnetic end effect (underheating or overheating of the billet).

5. The Induction Heating Experiments

5.1 Experimental Procedure

For the thixoforming process, the billet must be reheated to a semisolid state. The reheating process is very important in the forming process of an SSM billet; the process is not only necessary to achieve the required SSM billet state, but also to control the microstructure of the billet.

The SSM used in this study was A356 alloys fabricated by electromagnetic stirring, made by PECHINEY (Voreppe, France). This SSM is a casting alloy used in the manufacture of automotive parts. Its chemical composition is shown in Table 4, and the microstructure of the raw material is shown in Fig. 1.

A356 alloys fabricated by electromagnetic stirring are machined to $d \times l = 76 \times 90$ mm. The induction heating experiments were performed by using an induction heating system with a capacity of 50 kW. As shown in Fig. 2, to achieve uniform heating, the heating coil of the induction heating system was made by machining to $D_o \times H = 120 \times 120$ mm.[4,12,13] Thermocouple holes to measure the temperature accurately are machined to 3 mm diameter at the position of 45 mm from the surface of the billet and 3 mm diameter at the position of 10 mm from the lateral of the billet. To accurately control the temperature of the SSM, K-type CA thermocouples of φ 1.6 mm are inserted into the billet. Thermocouples are calibrated using 100 °C water. The accuracy of thermocouples is approximately 0.2%. A data logger TDS-302 (Tokyo Sokki Kenkyuio Co., Ltd., Tokyo) was used to receive the data, and the heating temperature was set to the data as a thermocouple position (b) in Fig. 2.

The reheating experiments were performed for the conditions in Table 5. The meanings of the symbols used in Table 5 are the same as those shown in Fig. 3.

5.2 Results and Discussion

The microstructure of SSMs after reheating must be a globular one. Moreover, when the SSM is fed from the induction heating system to the die, the shape of the SSM must be maintained. Therefore, the capacity of the induction heating system (Q), reheating time (t_a), holding temperature (T_h), holding time (t_h), reheating step, and adiabatic material size were considered as

Table 3 Designed dimensions of induction heating device (f = 60 Hz, dc = 10.7 mm,[16] l = 90 mm)

Billet diameter (d, mm)	Coil inner diameter (D_i, mm)	Minimum heating length (l_{kj}, mm)	Optimal coil length (H, mm)
76	100	93	18–168

Table 4 Chemical composition of A356

Content	Si	Fe	Cu	Mn	Mg	Cr	Zn	Ti	Pb
Min (%)	6.5	. . .	. . .	. . .	0.30	. . .	. . .	. . .	. . .
Max (%)	7.5	0.15	0.03	0.03	0.40	. . .	0.05	0.20	0.03

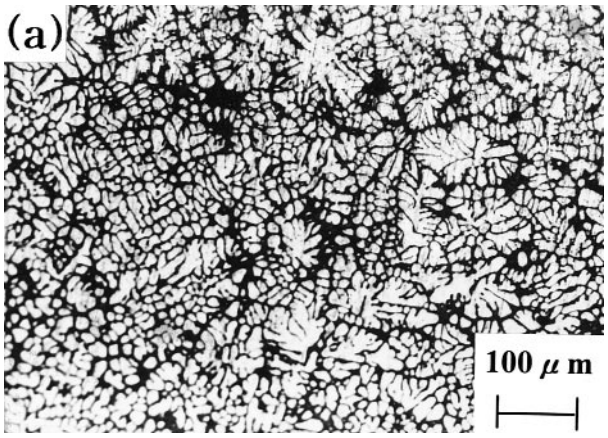

Fig. 1 Optical micrograph of raw A356 (ALTHIX)

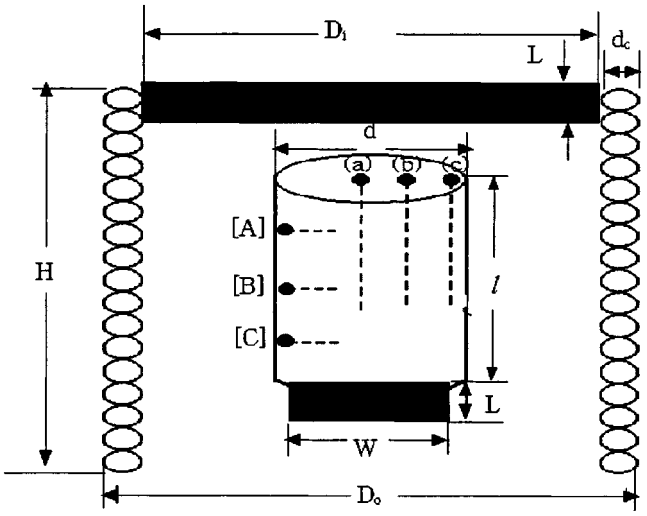

Fig. 2 Schematic illustration of induction heating of cylindrical billet

Table 5 Experimental conditions for the reheating of semisolid aluminum alloy (A356). Test billet size: $d \times l = 76 \times 90$ mm

Number	Reheating time t_a (min)			Holding temperature T_h(°C)			Holding time t_h (min)			Total time (min)	Capacity Q (kW)	Adiabatic material size (mm) $D \times W \times L$
	t_{a1}	t_{a2}	t_{a3}	T_{h1}	T_{h2}	T_{h3}	t_{h1}	t_{h2}	t_{h3}			
1	4	4	2	350	575	584	1	3	2	16	3.00	Without
2	4	4	2	350	575	584	1	3	2	16	3.30	Without
3	4	4	2	350	575	584	1	3	2	16	4.94	Without
4	4	4	2	350	575	584	1	3	2	16	6.30	Without
5	4	4	2	350	575	584	1	3	2	16	7.00	Without
6	4	4	2	350	575	584	1	3	2	16	7.50	Without
7	4	4	2	350	575	584	1	3	2	16	7.796	Without
8	4	4	2	350	575	584	1	3	2	16	8.398	Without
9	4	4	2	350	575	584	1	3	2	16	8.398	75 × 70 × 19
10	10	...	...	584	...	...	2	...	...	12	7.796	75 × 70 × 19
11	10	...	...	584	...	...	2	...	...	12	8.398	53 × 53 × 19
12	8	1	...	575	584	...	3	2	...	14	8.398	53 × 53 × 19
13	4	3	1	350	575	584	1	3	2	14	8.398	53 × 53 × 19
14	4	3	1	350	575	584	1	3	1	13	8.398	53 × 53 × 19
15	4	3	2	350	575	584	1	2	1	13	8.398	53 × 53 × 19
16	4	3	2	350	560	584	1	3	1	14	8.398	53 × 53 × 19
17	4	3	2	350	560	584	1	2	2	14	8.398	53 × 53 × 19
18	3	3	2	350	565	584	1	3	2	14	8.398	53 × 53 × 19
19	4	4	2	350	565	584	1	3	2	16	8.398	53 × 53 × 19
20	4	3	1	350	575	584	1	3	3	15	8.398	53 × 53 × 19
21	4	4	2	350	575	584	1	3	2	16	8.398	53 × 53 × 19
22	4	3	1	350	570	576	1	3	2	14	8.398	53 × 53 × 19
23	4	3	1	350	570	576	1	3	2	14	9.174	53 × 53 × 19
24	4	3	1	350	570	576	1	3	2	14	10.376	53 × 53 × 19
25	4	3	1	350	570	576	1	3	2	14	11.44	53 × 53 × 19
26	4	3	1	350	570	576	1	3	2	14	12.04	50 × 50 × 20
27	4	3	1	350	570	576	1	3	1	13	12.04	50 × 50 × 20
28	4	3	1	350	570	578	1	3	2	14	12.04	50 × 50 × 20

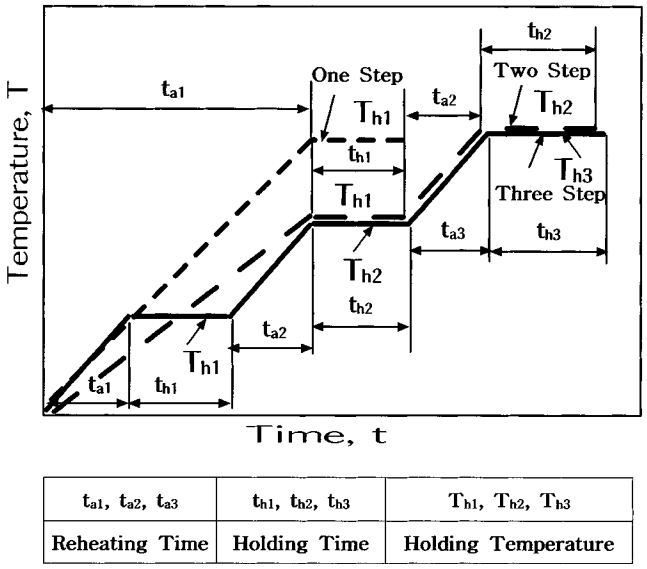

Fig. 3 Input data diagram of reheating conditions to obtain a fine globular microstructure

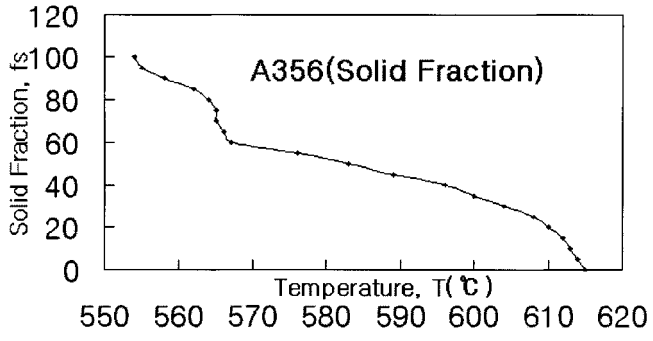

Fig. 4 Relationships between temperature and solid fraction for A356 (ALTHIX)

parameters of the experiment to observe the globularization of the microstructure and a small temperature gradient.

To determine the heating temperature of the SSM, the solid fraction of A356 alloys is used as a reference.[18] The relationship between temperature and the solid fraction of A356 alloys is given in Fig. 4. As shown in Fig. 4, the solid fraction of ALTHIX is changed rapidly at about 565 °C, which is lower (up to 10 °C) than the complete eutectic remelting temperature of 575 °C,[4,5,9,12,13,19,20] According to the Ref 18, the temperatures corresponding to the solid fraction of 50 and 55% are 584 and 576 °C, respectively.

For experiments 1 to 21, the reheating experiments were performed for *fs* = 50%. For experiments 1 to 9, the experiments were carried out at the reheating conditions t_{a1} = 4 min, t_{a2} = 4 min, t_{a3} = 2 min, t_{h1} = 1 min, t_{h2} = 3 min, t_{h3} = 2 min, T_{h1} = 350 °C, T_{h2} = 575 °C, and T_{h3} = 584 °C, but with a changing capacity of the induction heating system to determine the optimal capacity, by varying the heating time. In the case of the capacities (Q) of 7.796 and 8.398 kW, the billets reach the set temperature with a small temperature difference.

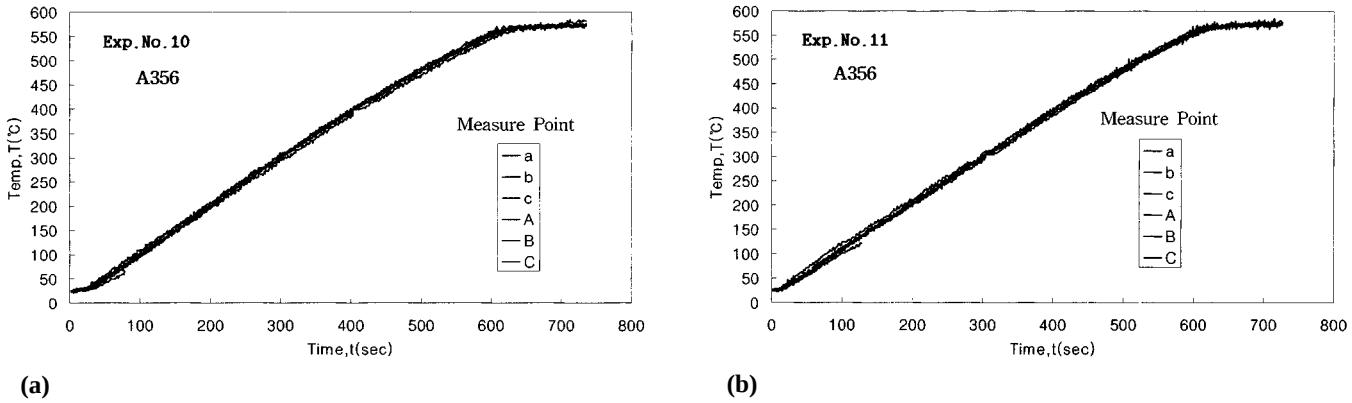

(a) **(b)**

Fig. 5 Temperature distribution in one-step reheating process of semisolid alloy ($f_s = 50\%$, $t_{a1} = 10$ min, $T_{h1} = 584$ °C, and $t_{h1} = 2$ min): **(a)** $Q = 7.796$ kW and **(b)** $Q = 8.398$ kW

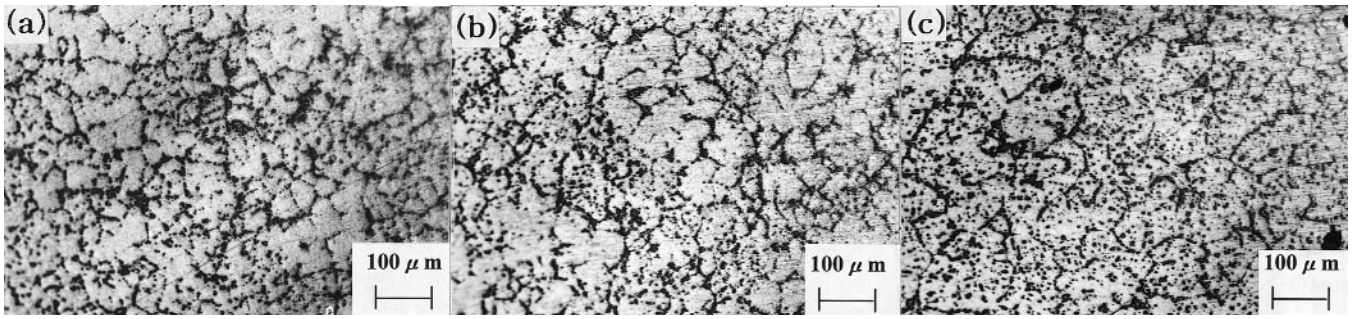

(a)

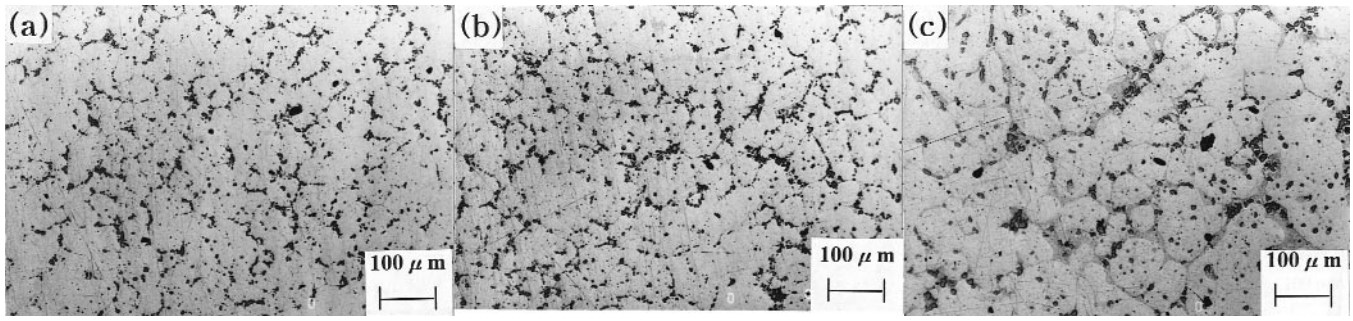

(b)

Fig. 6 Microstructure in one-step reheating process of semisolid aluminum alloy (A356, $f_s = 50\%$, $t_{a1} = 10$ min, $T_{h1} = 584$ °C, and $t_{h1} = 2$ min): **(a)** experiment 10, $Q = 7.796$ kW; and **(b)** experiment 11, $Q = 8.398$ kW

Therefore, experiments 10 and 11 were performed under the conditions $t_{a1} = 10$ min, $t_{h1} = 2$ min, and $T_{h1} = 584$ °C, with the capacities (Q) of 7.796 and 8.398 kW. For experiments 10 and 11, the sizes of adiabatic materials are $D \times W \times L = 75 \times 70 \times 19$ mm and $D \times W \times L = 53 \times 53 \times 19$ mm, respectively. Figure 5 and 6 show the temperature distribution and microstructure of reheated SSMs for experiments 10 and 11. The temperature difference of the reheated SSM at the measured positions is small, the particle size is also generally small, and the globular microstructure is not obtained. Due to the lack of sufficient holding time for the separation between solid and liquid before and after the phase change, and for globularization of the solid particle, one-step reheating is unsuitable for the billet size of $d \times l = 76 \times 90$ mm.

Experiment 12 was performed under the conditions $t_{a1} = 8$ min, $t_{a2} = 1$ min, $t_{h1} = 3$ min, $t_{h2} = 2$ min, $T_{h1} = 575$ °C, $T_{h2} = 584$ °C, and $Q = 8.398$ kW. Moreover, the size of the adiabatic material is $D \times W \times L = 53 \times 53 \times 19$ mm. Figure 7 and 8 show the temperature distribution and microstructure of the reheated SSM for experiment 12. The temperature difference of reheated SSMs at the measured positions is small, and a good globular microstructure is obtained at positions (a), (b), and (c) in Fig. 2.

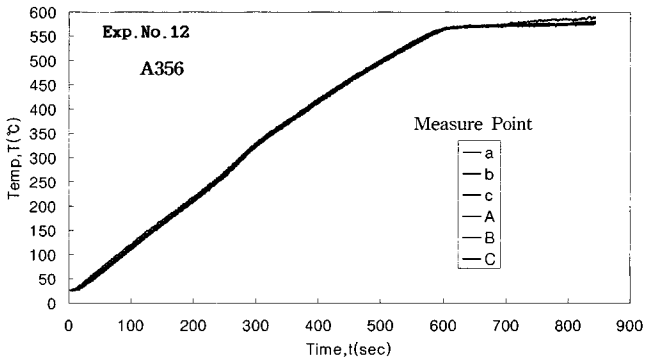

Fig. 7 Temperature distributions in two-step reheating process of semi-solid alloy ($f_s = 50\%$, $t_{a1} = 8$ min, $t_{a2} = 1$ min, $T_{h1} = 575$ °C, $T_{h2} = 584$ °C, $t_{h1} = 3$ min, $t_{h2} = 2$ min, and $Q = 8.398$ kW

The accuracy of globularization of position (c) is similar to (a) and (b), but the microstructure of position (c) is coarse.

Experiment 13 was performed under the conditions $t_{a1} = 4$ min, $t_{a2} = 3$ min, $t_{a3} = 1$ min, $t_{h1} = 1$ min, $t_{h2} = 3$ min, $t_{h3} = 2$ min, $T_{h1} = 350$ °C, $T_{h2} = 575$ °C, $T_{h3} = 584$ °C, and 8.398 kW. The size of the adiabatic material is $D \times W \times L = 53 \times 53 \times 19$ mm. Figures 9 and 10 show the temperature distribution and microstructure of reheated SSMs for experiment 13. The temperature difference of reheated SSMs at the measured positions is small, and a fine globular microstructure is obtained at positions (a), (b), and (c) in Fig. 2.

Comparing experiments 12 and 13, the temperature difference of reheated SSMs at the measured positions is small. The microstructure of experiment 13 (three-step reheating) is finer and more globular than that of experiment 12 (two-step reheating).

Experiments 14 and 20 were performed under the same conditions as experiment 13 $t_{h3} = 1$ min and $t_{h3} = 3$ min, respectively. Figure 9 and 10 show the temperature distribution and microstructure of the reheated SSMs for experiments 13, 14, and 20. The temperature difference of reheated SSMs at the measured positions is small. For experiment 14, the microstructure is not globular at positions (a) and (b) in Fig. 2, and the globularization is in progress at position (c). Experiment 20 shows good globularization, but the size of the globularization is large at positions (a), (b), and (c) in Fig. 2.

Experiments 19 and 21 were performed at $T_{h2} = 565$ °C and $T_{h2} = 575$ °C. Figure 11 and 12 show the temperature distribution and microstructure of reheated SSMs for experiments 19 and 21. In the case of experiment 19, the microstructure of globularization was not obtained at position (a) in Fig. 2, globularization was in progress at position (b), and a fine globular microstructure was observed at position (c). In the case of experiment 21, the temperature difference of the reheated SSM at the measured positions is larger than that of experiment 19. Experiment 21 shows good globularization, but shows cohesion between solid regions at positions (a), (b), and (c) in Fig. 2.

For experiments 22 to 28, the reheating experiments were performed for $f_s = 55\%$. Experiments 22 to 26 were carried out under the reheating conditions $t_{a1} = 4$ min, $t_{a2} = 3$ min, $t_{a3} = 1$ min, $t_{h1} = 1$ min, $t_{h2} = 3$ min, $t_{h3} = 2$ min, $T_{h1} = 350$ °C , $T_{h2} = 570$ °C, and $T_{h3} = 576$ °C, changing the capacity of the induction heating system to determine the optimal capacity, by varying the heating time. The sizes of adiabatic materials are $D \times W \times L = 53 \times 53 \times 19$ mm for experiments 22 to 25 and $D \times W \times L = 50 \times 50 \times 20$ mm for experiment 26, respectively. In the case of $Q = 12.04$ kW, the billet reaches the set temperature with a small temperature difference.

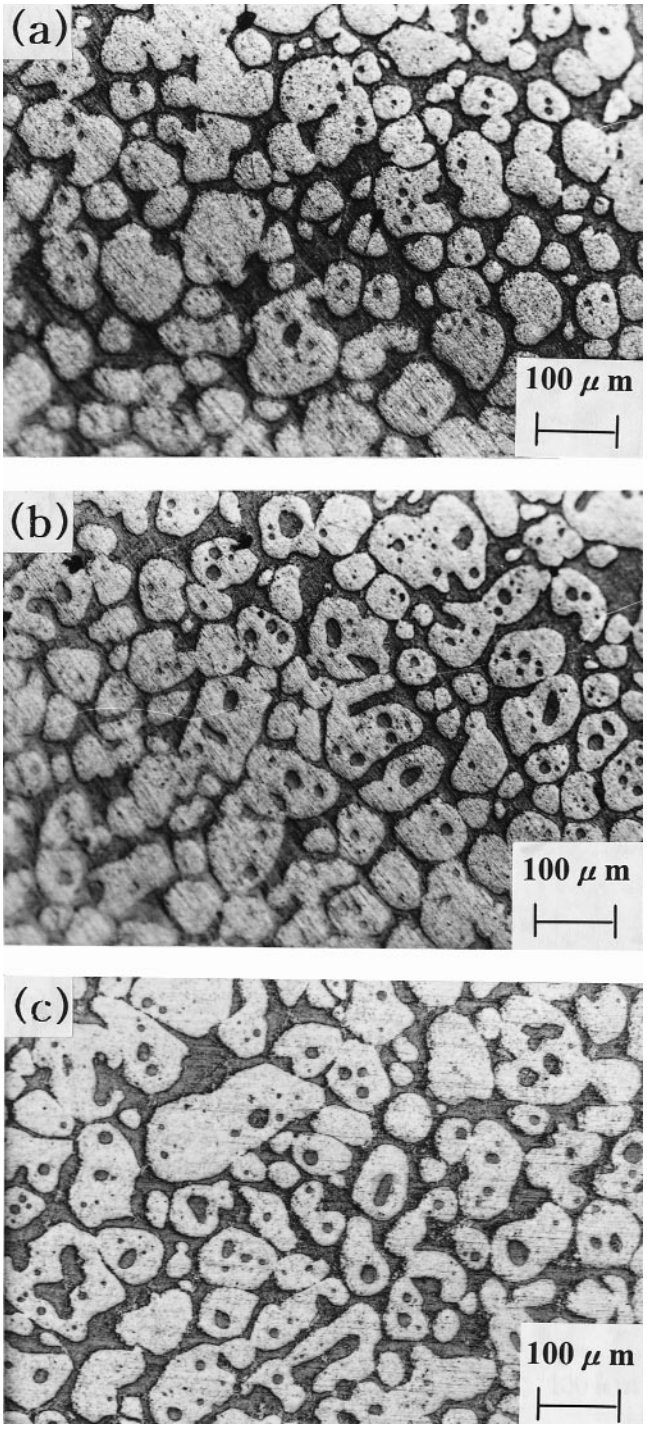

Fig. 8 **(a)** to **(c)** Microstructure in two-step reheating process of semi-solid aluminum alloy (experiment 12, A356, $f_s = 50\%$, $t_{a1} = 8$ min, $t_{a2} = 1$ min, $T_{h1} = 575$ °C, $T_{h2} = 584$ °C, $t_{h1} = 3$ min, $t_{h2} = 2$ min, and $Q = 8.398$ kW)

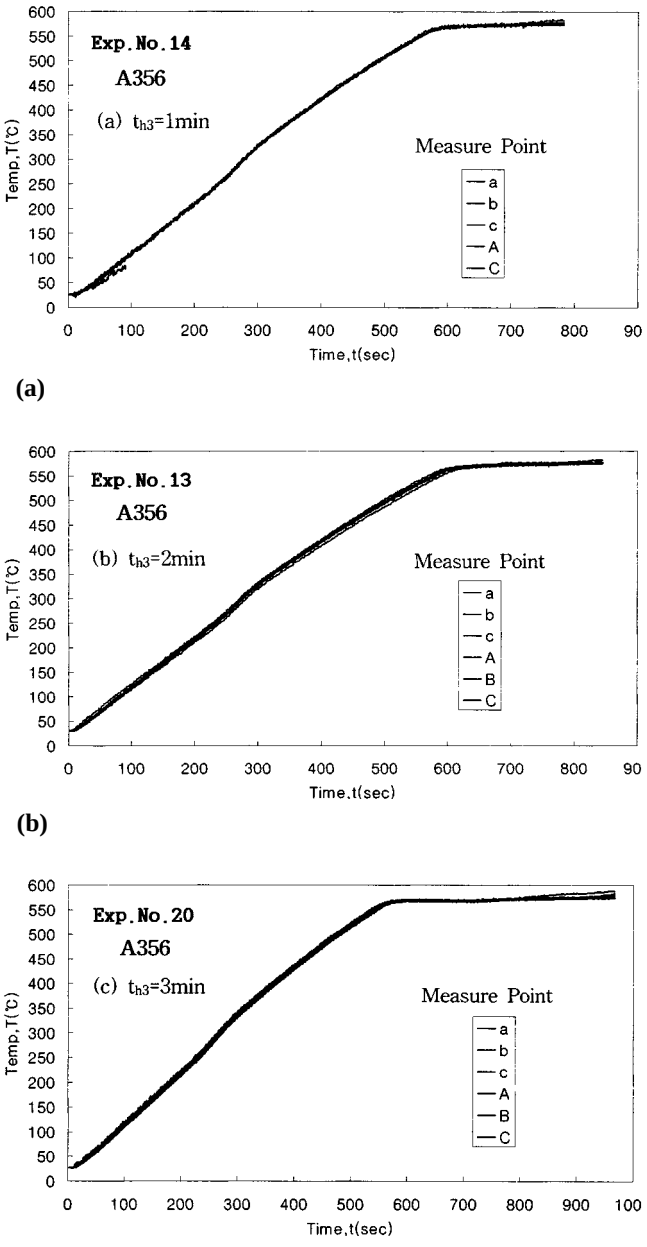

Fig. 9 **(a)** to **(c)** Temperature distributions in three-step reheating process of semisolid alloy ($f_s = 50\%$, $t_{a1} = 4$ min, $t_{a2} = 3$ min, $t_{a3} = 1$ min, $T_{h1} = 350$ °C, $T_{h2} = 575$ °C, $T_{h3} = 584$ °C, $t_{h1} = 1$ min, $t_{h2} = 3$ min, and $Q = 8.398$ kW)

The reheating experiments 26 and 27 were performed at $t_{h3} = 2$ min and $t_{h3} = 1$ min. Figure 13 and 14 show the temperature difference of the reheated SSM for experiments 26 and 27. The temperature difference of the reheated SSM at the measured positions is small, but the shooting phenomenon is observed at position [C] of Fig. 2. It was found that, due to the slightly high capacity at position [C] in Fig. 2, the billet overheated instantaneously. Moreover, in this study, it was found that, because the shooting phenomenon occurs at low temperature ranges and short time intervals, it does not affect the solid fraction. In the case of experiment 26, a fine globular microstructure was obtained at positions (a), (b), and (c). However, in the case of experiment 27, the globular microstructure was not obtained at positions (a) and (b). Due to the separation between solid and liquid, and the globularization of the solid before and after the phase change, the globularization is in progress at position (c) of Fig. 2. Compared to experiment 26, experiment 27 is due to the lack of sufficient holding time for the separation between solid and liquid before and after phase change and for globularization of the solid particles.

5.3 Differences Between the Solid Fractions 50 and 55%

For $f_s = 50$ and 55%, it was found that the higher the solid fraction, the worse the degree of globularization, but the boundary between the solid regions and the liquid regions is clear.[2–4,12]

Figure 15 shows the micrographs magnified 1000 times to observe the eutectic microstructure of experiments 13 and 26, which achieved the finest globular microstructure for $f_s = 50$ and 55%. Figure 16 shows the surface roughness after water quenching. (a) and (b) in Fig. 15 show that the eutectic is melted completely. Therefore, the A356 (ALTHIX) alloy is held without a change of temperature at around 575 °C, which is the eutectic temperature for 120 to 130 s. And the solid fraction is then rapidly changed, because of the melting of the eutectic in this temperature range. It was found that the eutectic is melted completely at over 575 °C, and complete eutectic melting is necessary to obtain a fine globular microstructure. The temperature rise does not occur until sufficient thermal energy is provided to melt the eutectic, because much thermal energy and time are necessary to melt the eutectic.[2–5,12,13] Before and after the melting of the eutectic, the solid fraction is rapidly changed, and a rapid temperature rise occurs when the eutectic is melted. Due to this temperature rise, the temperature difference becomes large, and controlling the reheating temperature is difficult. Therefore, to homogeneously control the temperature distribution and the solid fraction of the SSM, the billet must be reheated in three steps. As shown in (a) and (b) of Fig. 16, the surface roughness after water quenching of $f_s = 55\%$ is better than that of $f_s = 50\%$.

It was found that in the case of $d \times l = 76 \times 90$ mm (shown in Fig. 10), one-step reheating is not a good process, because the size of the solid particles is small, and the microstructure of globularization is not obtained. As shown in Fig. 8, 10, 12, and 14, three-step reheating is better than two-step reheating with respect to small solid particles and the degree of globularization.

The holding time of the final step is very important in the three-step reheating process.[2–5,12,13] As shown in Fig. 10(a) and 14(b), if the holding time of the final step is short, the microstructure of globularization is not obtained, due to the lack of sufficient holding time for the separation between a solid and a liquid, before and after phase change, and for globularization of the solid particles. On the other hand, if the holding time of the final step is too long, the microstructure becomes coarse, due to the cohesion of the solid regions and the decrease in the liquid regions, as shown in Fig. 10(c). Therefore, the optimal holding time of the final step to obtain a fine globular microstructure without agglomeration is 2 min.

This study can be compared to the reheating conditions performed with $d \times l = 39 \times 85$ mm and $d \times l = 76 \times 60$ mm by Kang *et al.*,[9] where the finest globular microstructure is obtained

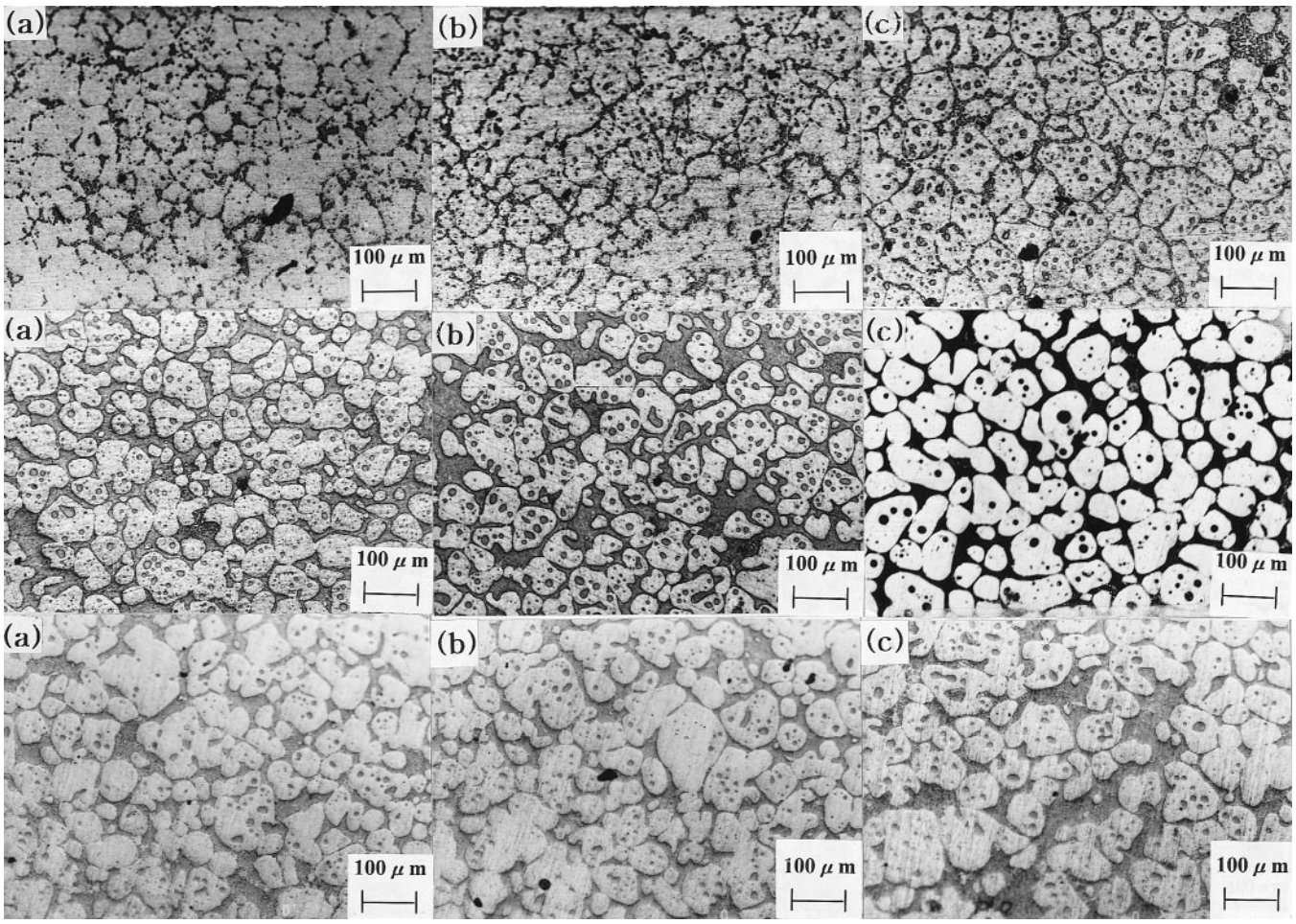

Fig. 10 **(a)** to **(c)** Microstructure in three-step reheating process of semisolid aluminum alloy (A356, $f_s = 50\%$, $t_{a1} = 4$ min, $t_{a2} = 3$ min, $t_{a3} = 1$ min, $T_{h1} = 350$ °C, $T_{h2} = 575$ °C, $T_{h3} = 584$ °C, $t_{h1} = 1$ min, $t_{h2} = 3$ min, and $Q = 8.398$ kW)

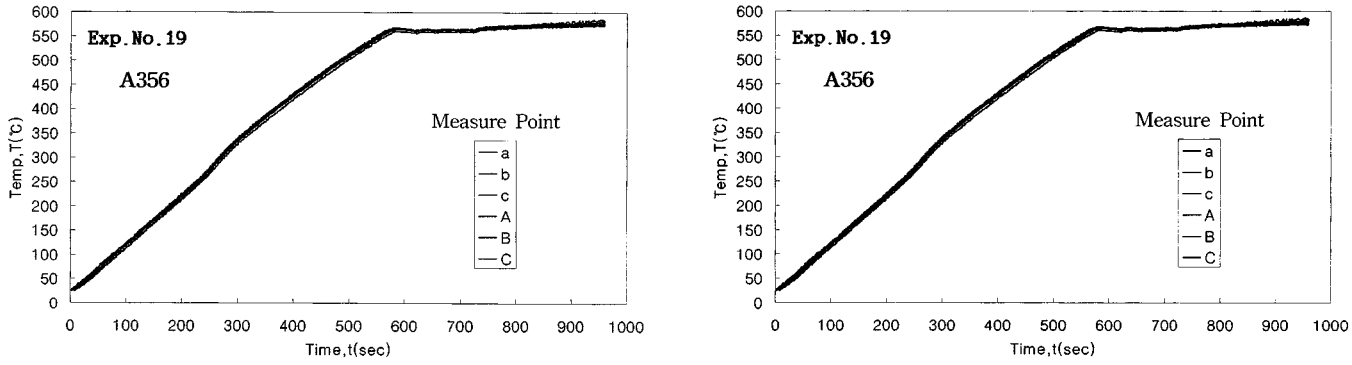

Fig. 11 Temperature distributions in three-step reheating process of semisolid alloy ($f_s = 50\%$, $t_{a1} = 4$ min, $t_{a2} = 4$ min, $t_{a3} = 2$ min, $T_{h1} = 350$ °C, $T_{h3} = 584$ °C, $t_{h1} = 1$ min, $t_{h2} = 3$ min, $t_{h3} = 2$ min, and $Q = 8.398$ kW): (a) $T_{h2} = 565$ °C, and (b) $T_{h2} = 575$ °C

under the one-step reheating process at $t_{a1} = 10$ min, $t_{h1} = 2$ min, $T_{h1} = 573$, and $Q = 3.3$ kW for $d \times l = 39 \times 85$ mm and under the two-step reheating process at $t_{a1} = 8$ min, $t_{a2} = 1$ min, $t_{h1} = 3$ min, $t_{h2} = 2$ min, $T_{h1} = 575$ °C, $T_{h2} = 584$ °C, and $Q = 3.00$ kW for $d \times l = 76 \times 60$ mm. In this study, the finest globular microstructure was obtained under the three-step reheating process at $t_{a1} = 4$ min, $t_{a2} = 3$ min, $t_{a3} = 1$ min, $t_{h1} = 1$ min, $t_{h2} = 3$ min, $t_{h3} = 2$ min, $T_{h1} = 350$ °C, $T_{h2} = 575$ °C, $T_{h3} = 584$ °C, $Q = 8.398$ kW, with the size of the adiabatic material being $D \times W \times L = 53 \times 53 \times 19$ mm for $f_s = 50\%$, and under the three-step reheating process at $t_{a1} =$

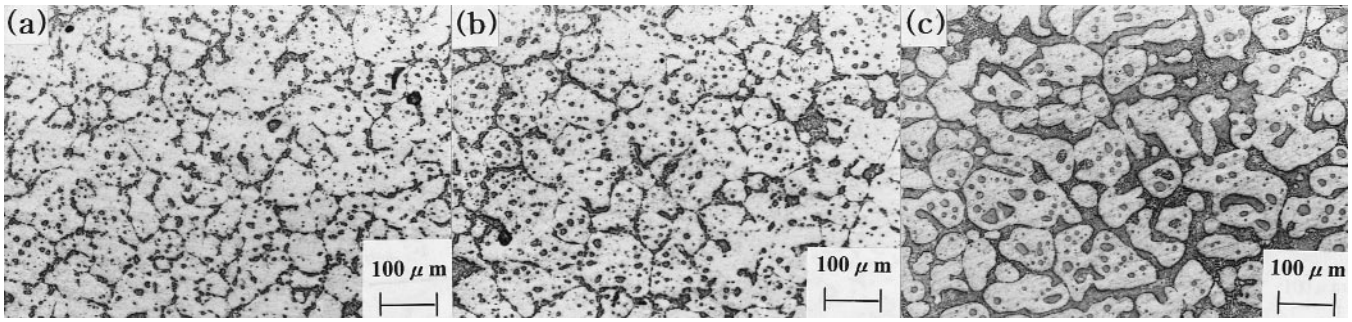

(a)

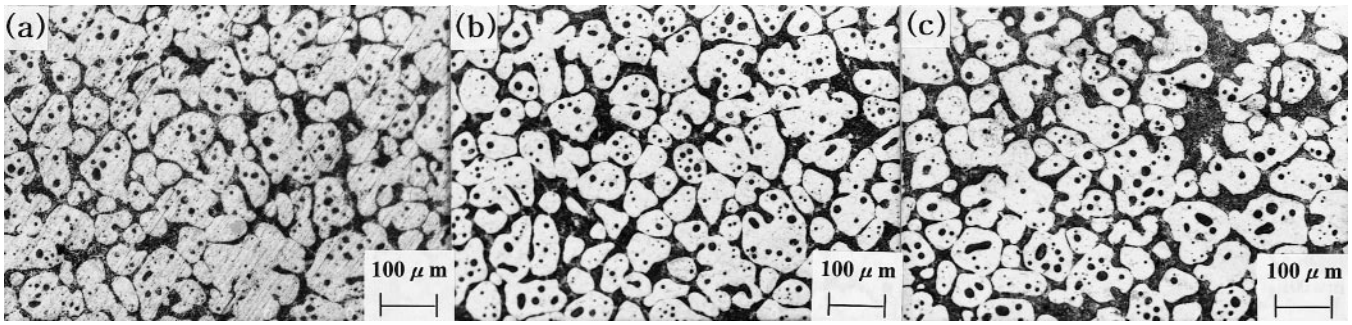

(b)

Fig. 12 Microstructure in three-step reheating process of semisolid aluminum alloy (A356, $f_s = 50\%$, $t_{a1} = 4$ min, $t_{a2} = 4$ min, $t_{a3} = 2$ min, $T_{h1} = 350$ °C, $t_{h3} = 584$ °C, $t_{h1} = 1$ min, $t_{h2} = 3$ min, $t_{h3} = 2$ min, and $Q = 8.398$ kW). **(a)** experiment 19, $T_{h2} = 565$ °C; and **(b)** experiment 21, $T_{h2} = 575$ °C

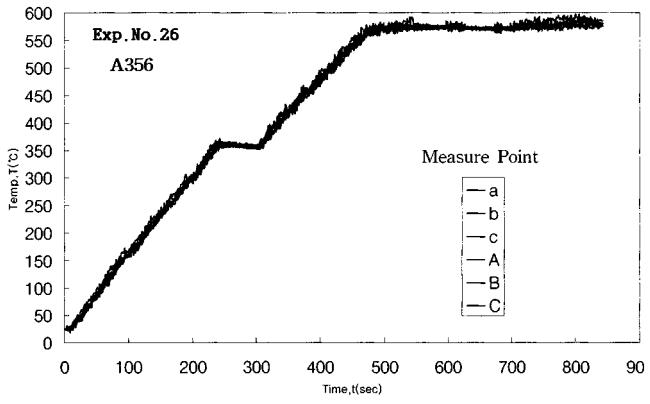

(a)

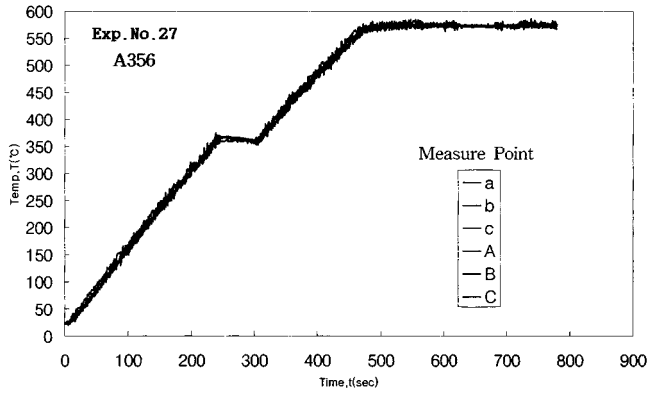

(b)

Fig. 13 Temperature distributions in three-step reheating process of semisolid alloy ($f_s = 55\%$, $t_{a1} = 4$ min, $t_{a2} = 3$ min, $t_{a3} = 1$ min, $T_{h1} = 350$ °C, $T_{h2} = 570$ °C, $T_{h3} = 576$ °C $t_{h1} = 1$ min, $t_{h2} = 3$ min, and $Q = 12.04$ kW): **(a)** $T_{h3} = 2$ min, and **(b)** $T_{h3} = 1$ min

4 min, $t_{a2} = 3$ min, $t_{a3} = 1$ min, $t_{h1} = 1$ min, $t_{h2} = 3$ min, $t_{h3} = 2$ min, $T_{h1} = 350$ °C, $T_{h2} = 570$ °C, $T_{h3} = 576$ °C, and $Q = 12.04$ kW, with the size of the adiabatic material being $D \times W \times L = 50 \times 50 \times 20$ mm for the solid fraction of $f_s = 55\%$.

This study shows that, the larger the billet size, the better the multistep reheating compared with reported results, and the heating time and the capacity of the induction heating system must be increased.

In the present study, since a fine and completely melted eutectic Si phase of A356 was obtained, it is expected that during thixoforming, products with good mechanical properties will be manufactured.

Many lead times for manufacturing complexly shaped parts by the net shape metal forming process such as thixoforming or semisolid forming are required due to the time for die design, induction heating, and the forming process. In order to reduce these lead times, many numerical simulation codes have been developed to analyze the required net shape metal forming processes. However, there have not been any published reports that adapt these codes to the specific characteristics[21] of SSMs.

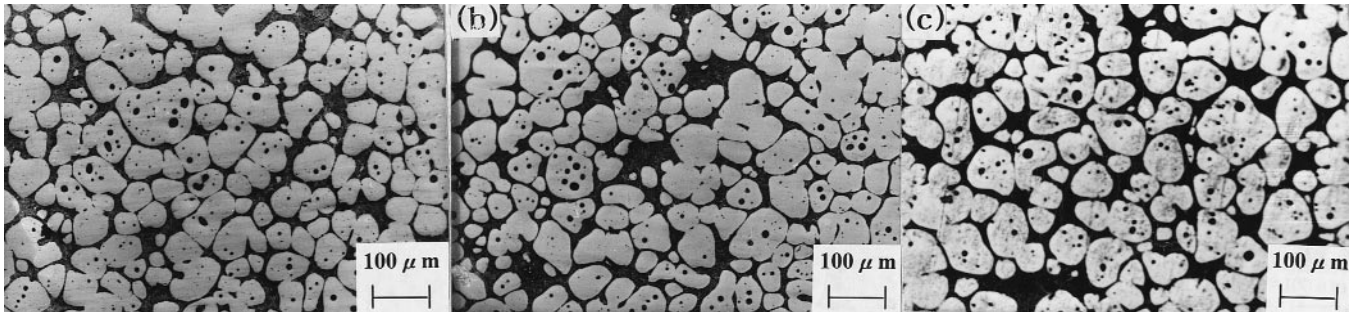

(a)

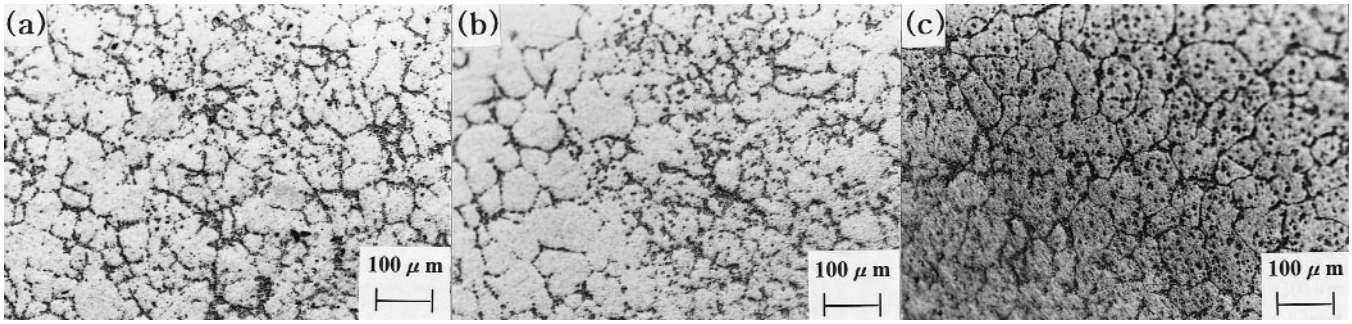

(b)

Fig. 14 Microstructure in three-step reheating process of semisolid aluminum alloy (A356, $f_s = 55\%$, $t_{a1} = 4$ min, $t_{a2} = 3$ min, $t_{a3} = 1$ min, $T_{h1} = 350$ °C, $T_{h2} = 570$ °C, $T_{h3} = 576$ °C, $t_{h1} = 1$ min, $t_{h2} = 3$ min, and $Q = 12.04$ kW): **(a)** experiment 26, $t_{h3} = 2$ min; and **(b)** experiment 27, $t_{h3} = 1$ min

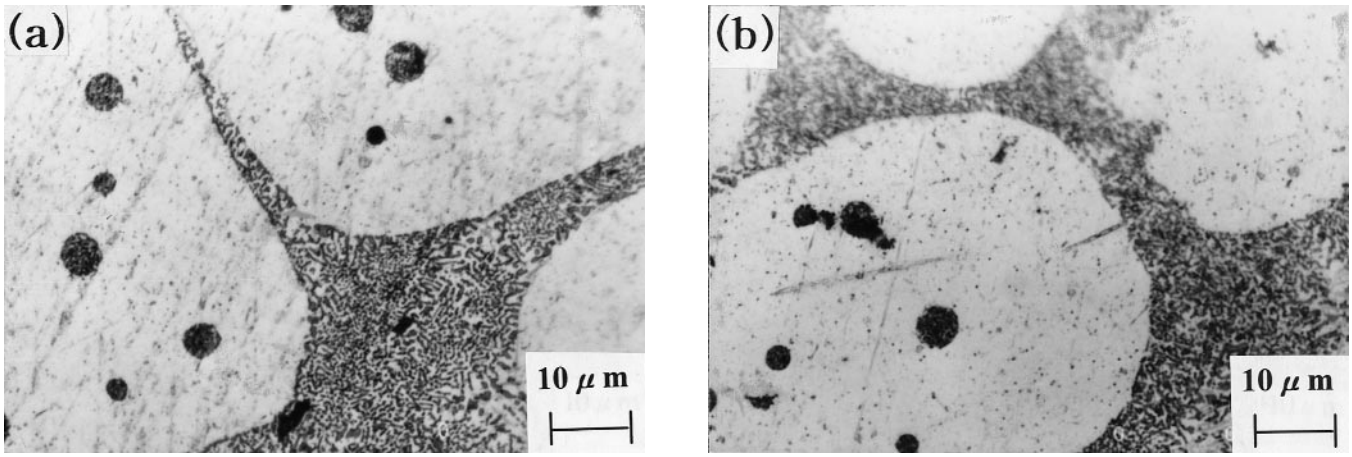

Fig. 15 Eutectic microstructure of semisolid A356 alloy (ALTHIX). **(a)** Experiment 13, $f_s = 50\%$, $t_{a1} = 4$ min, $t_{a2} = 3$ min, $t_{a3} = 1$ min, $T_{h1} = 350$ °C, $T_{h2} = 575$ °C, $T_{h3} = 584$ °C, $t_{h1} = 1$ min, $t_{h2} = 3$ min, $t_{h3} = 2$ min, and $Q = 8.398$ kW. **(b)** Experiment 26, $f_s = 55\%$, $t_{a1} = 4$ min, $t_{a2} = 3$ min, $t_{a3} = 1$ min, $T_{h1} = 350$ °C, $T_{h2} = 570$ °C, $T_{h3} = 576$ °C, $t_{h1} = 1$ min, $t_{h2} = 3$ min, $t_{h3} = 2$ min, and $Q = 12.04$ kW

SEMI-FORM S/W for simulation of the thixoforming process is currently under development.[22]

6. Conclusions

This paper has presented all of the induction heating processes from the optimal coil design for uniform heating to the conrol of globular microstructure to prevent coarsening phenomena during induction heating. The results are summarized as follows.

- For the A356 billet with $d \times l = 76 \times 90$ mm (the frequency of the commercial induction heating system: 60 Hz) often used in the thixoforming process, the optimal coil dimensions for uniform induction heating were proposed.
- This study shows that, the larger the billet size, the better the multistep reheating compared with reported results, and the

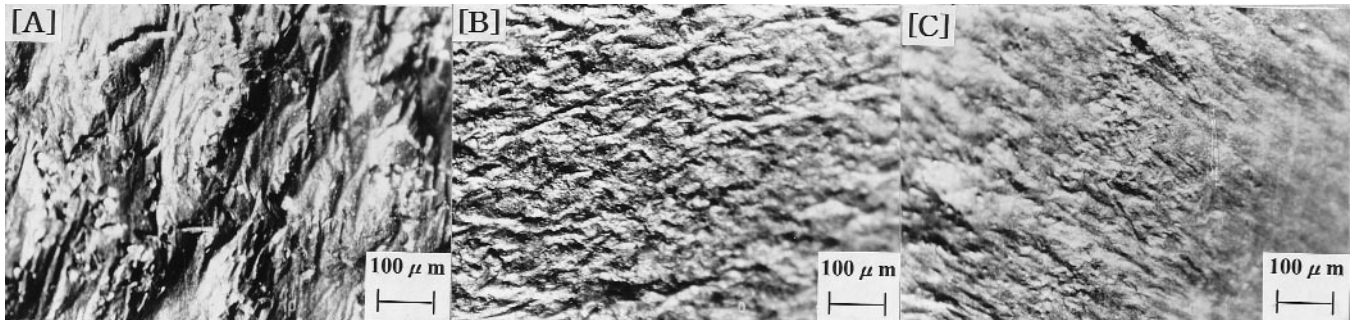

(a)

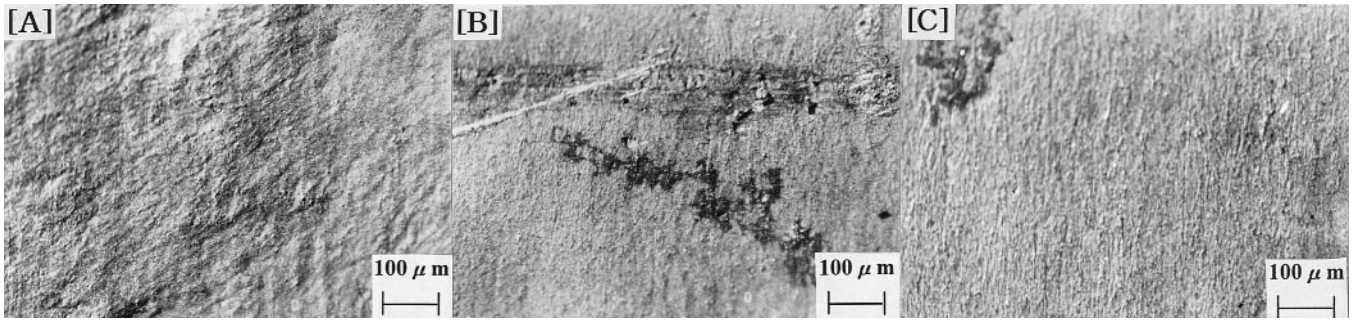

(b)

Fig. 16 Surface roughness of specimen after water quenching. **(a)** Experiment 13, f_s = 50%, t_{a1} = 4 min, t_{a2} = 3 min, t_{a3} = 1 min, T_{h1} = 350 °C, T_{h2} = 575 °C, T_{h3} = 584 °C, t_{h1} = 1 min, t_{h2} = 3 min, t_{h3} = 2 min, and Q = 8.398 kW. **(b)** Experiment 26, f_s = 55%, t_{a1} = 4 min, t_{a2} = 3 min, t_{a3} = 1 min, T_{h1} = 350 °C, T_{h2} = 570 °C, T_{h3} = 576 °C, t_{h1} = 1 min, t_{h2} = 3 min, t_{h3} = 2 min, and Q = 12.04 kW

heating time and the capacity of the induction heating system must be increased.

- We could see that the final holding time of 2 min is suitable to maintain a globular microstructure.
- In the reheating process of the SSM with $d \times l$ = 76 × 90 mm, because three-step reheating produces the best globular fine microstructure, it is more suitable than two-step reheating.
- In the case of the three-step reheating process, if the reheating holding time of the final step is too short, a globular microstructure cannot be obtained, and, if the holding time is too long, the risks of grain coarsening may be increased. A fine globular microstructure is obtained by using a holding time of 2 min in the three-step reheating process.

Acknowledgments

This work has been supported by the Engineering Research Center for Net Shape and Die Manufacturing (ERC/NSDM), which is financed jointly by the Korean Science and Engineering Foundation (KOSEF).

References

1. D.H. Kirkwood: *Int. Mater. Rev.*, 1994, vol. 39 (5), pp. 173-89.
2. H.K. Jung and C.G. Kang: *Metall. Mater. Trans. A*, 1999, vol. 30A, pp. 2967-77.
3. H.K. Jung and C.G. Kang: *J. Kor. Foundrymen's Soc.*, 1999, vol. 19 (3), pp. 225-35.
4. C.G. Kang, H.K. Jung, and Y.J. Jung: *Proc. 6th Int. Conf. on Technology of Plasticity (6th ICTP)*, Nuremberg, 1999, M. Geiger, ed., University of Erlangen-Nuremberg, Nuremberg, Germany, 1999, pp. 1689-94.
5. C.G. Kang, Y.H. Kim, and H.K. Jung: "Thixoforming Process Development of Aluminum Materials," *Technical Report*, Engineering Research Center for Net Shape and Die Manufacturing, Pusan National University, Pusan, Korea, 1999.
6. K.P. Young and R. Fitze: *Proc. 3rd Int. Conf. on Semi-Solid Processing of Alloys and Composites*, Tokyo, 1994, M. Kiuchi, ed., Tokyo University, Tokyo, Japan, 1994, pp. 155-77.
7. P. Kapranos, R.C. Gibson, D.H. Kirkwood, and C.M. Sellars: *Proc. 4th Int. Conf. on Semi-Solid Processing of Alloys and Composites*, Sheffield, 1996, D.H. Kirkwood and P. Kapranos, eds., The University of Sheffield, UK, 1996, pp. 148-52.
8. W. Kahrmann, R. Schragner, and K. Young: *Proc. 4th Int. Conf. on Semi-Solid Processing of Alloys and Composites*, Sheffield, 1996, D.H. Kirkwood and P. Kapranos, eds. The University of Sheffield, UK, 1996, pp. 154-58.
9. C.G. Kang, J.C. Choi, B.M. Kim, H.J. Park, H.K. Jung, and J.H. Park: "Development of Compound Forging Technology of Semi-Solid Materials and Its Commercialization," *Technical Report*, Engineering Research Center for Net Shape and Die Manufacturing, Pusan National University, Pusan, Korea, 1998.
10. G. Clauser, A. Ravaioli, F. Ciselli, and M. Vassallo: *Proc. 4th lnt. Conf. on Semi-Solid Processing of Alloys and Composites*, Sheffield, 1996, D.H. Kirkwood and P. Kapranos, eds., The University of Sheffied, UK, 1996, pp. 234-38.
11. T. Witulski, A. Winkelmann, and G. Hirt: *Proc. 4th Int. Conf. on Semi-Solid Processing of Alloys and Composites*, Sheffield, 1996,

D.H. Kirkwood and P. Kapranos, eds., The University of Sheffield, UK, 1996. pp. 242-46.
12. H.K. Jung and C.G. Kang: *J. Kor. Foundrymen's Soc.*, 1998, vol. 18 (5), pp. 450-61.
13. C.G. Kang, H.K. Jung, K.D. Jung, and D.H. Lee: *Proc. Korea-French Int. Joint Workshop on Metal Forming*, Daejon, 1999, D.Y. Yang, ed., KAIST, Daejon, Korea, 1999, pp. 51-56.
14. E.J. Davies: *Conduction and Induction Heating*, Peter Peregrinus Ltd., London, 1990, pp. 100-222.
15. N.R. Stansel: *Induction Heating*, McGraw-Hill, New York, NY, 1949, pp. 178.
16. V.I. Rudnev, L.C. Raymond, D.L. Loveless, and M.R. Black: *Induction Heat Treatment*, Marcel Dekker. Inc., New York, NY, 1997, pp. 775-911.
17. *Metals Handbook*, 10th ed., ASM International, Materials Park, OH, 1990, vol. 2, pp. 164-66.
18. G. Hirt, R. Cremer, A. Winkelmann, T. Witulski, and M. Zillgen: *J. Mater. Processing Technol.*, 1994, vol. 45, pp. 359-64.
19. W.R. Loué and M. Garat: *Proc. Symp. on Forming Technology of Semi-Solid Metals*, Pusan, 1997, C.G. Kang, ed., Pusan National University, Pusan, Korea, 1997, pp. 96-104.
20. C. Pluchon, W.R. Loué, and M. Garat: *Proc. Symp. on Forming Technology of Semi-Solid Metals*, Pusan, 1997, C. G. Kang, ed., Pusan National University, Pusan, Korea, 1997, pp. 80-95.
21. C.G. Kang, H.K. Jung, and N.S. Kim: *Int. J. Mech. Sci.*, 1999, vol. 41 (12), pp. 1423-45.
22. N.S. Kim, H.K. Jung, and C.G. Kang: *Proc. 1999 Korean Society of Precision Engineering Spring Conf.*, Daegu, 1999, J. M. Lee, ed., Keimyung University, Daegu, Korea, 1999, pp. 604-07.